# (R)-11-Hydroxy- and (R)-11-Hydroxy-10-methylaporphine: Synthesis, Pharmacology, and Modeling of $D_{2A}$ and 5-$HT_{1A}$ Receptor Interactions

Martin H. Hedberg,[†] Anette M. Johansson,*[,†] Gunnar Nordvall,[†] Ari Yliniemelä,[†,‡] Hong Bing Li,[§] Arnold R. Martin,[§] Stephan Hjorth,[∥] Lena Unelius,[⊥] Staffan Sundell,[▽] and Uli Hacksell[†]

*Organic Pharmaceutical Chemistry, Uppsala University, Uppsala Biomedical Centre, Box 574, S-751 23 Uppsala, Sweden, VTT Chemical Technology, POB 1401, FIN-02044 VTT, Finland, Department of Pharmacology and Toxicology, College of Pharmacy, University of Arizona, Tucson, Arizona 85721, Departments of Pharmacology and Structural Chemistry, University of Göteborg, Medicinaregatan 7, S-413 90 Göteborg, Sweden, and Department of Molecular Pharmacology, CNS Preclinical R&D, Astra Arcus, S-151 85 Södertälje, Sweden*

*Received September 27, 1994*[⊗]

(R)-11-Hydroxyaporphine (**2**) and (R)-11-hydroxy-10-methylaporphine (**3**) were synthesized from natural morphine by using new, short, and efficient synthetic sequences. The dopaminergic and serotonergic effects of **2** and **3** were evaluated by use of *in vitro* and *in vivo* test systems. The results indicate that **3** is a potent, selective, and efficacious 5-$HT_{1A}$ receptor agonist. In contrast, **2** is a partial 5-$HT_{1A}$ receptor agonist of low potency which has affinity also for central $D_1$ and $D_{2A}$ receptors. The differences in pharmacological profiles were rationalized by modeling of ligand–receptor interactions using homology-based receptor models of the 5-$HT_{1A}$ and $D_{2A}$ receptor binding site. The selective and pronounced serotonergic effects of **3** appear to be due to the C10-methyl group, which is accommodated by a lipophilic pocket in the 5-$HT_{1A}$ receptor. In contrast, the C10-methyl group of **3** is not accommodated by the binding site model of the $D_{2A}$ receptor.

Small structural changes in aporphine derivatives may lead to drastic changes in pharmacological profiles. (R)-Apomorphine (**1**), which was first synthesized around 1869,[1] acts as an agonist on central dopamine (DA) $D_1$ and $D_2$ receptors.[2] In contrast, (R)-11-hydroxyaporphine (**2**) seems to be a $D_1$ receptor antagonist.[3] The monophenolic **2** has affinity for $D_2$ receptors but failed to display agonist activity in a serum prolactin assay indicating lack of agonist activity at $D_2$ receptors.[3] However, racemic **2** displayed $D_2$ agonist activity by inducing contralateral rotation in rats lesioned unilaterally with 6-hydroxydopamine.[4] Replacement of the C10-hydroxy group of **1** with a methyl group, providing **3**, produced a potent 5-hydroxytryptamine (5-$HT_{1A}$) receptor agonist which did not produce any dopaminergic effect in the cat cardiovascular nerve test.[5]

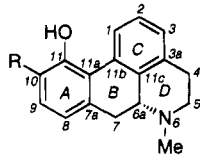


**1** R = OH
**2** R = H
**3** R = Me

In order to understand the differences in pharmacological profiles of **1**–**3**, we have resynthesized **2** and **3** from natural morphine by using new, short, and efficient synthetic sequences and the dopaminergic and serotonergic effects of the compounds have been evaluated by use of *in vitro* and *in vivo* test systems. The differences in pharmacological profiles have been rationalized by modeling of ligand–receptor interactions using homology-based receptor models of the 5-$HT_{1A}$ and $D_{2A}$ receptor binding site. The results indicate that **3** is a potent, selective, and efficacious 5-$HT_{1A}$ receptor agonist. In contrast, **2** is a partial 5-$HT_{1A}$ receptor agonist of low potency which has affinity also for central $D_1$ and $D_{2A}$ receptors. The selective and pronounced serotonergic effects of **3** can be rationalized by the 5-$HT_{1A}$ binding site model in which the C10-methyl group is accommodated by a lipophilic pocket, which is not present in the $D_{2A}$ binding site.

## Chemistry

**Synthesis.** Compounds **2** and **3** have previously been synthesized from natural (−)-morphine (**4**) in five[6] and seven[5] steps, respectively. The efficient methods used here for the synthesis of **2** and **3** are shown in Scheme 1 and were recently published.[7] The key intermediate, triflate **5**, can be utilized in two different routes to **2** and **3**: (a) a palladium-catalyzed reaction followed by an acid-catalyzed rearrangement reaction or (b) an acid-catalyzed rearrangement reaction followed by a palladium-catalyzed reaction.

In addition to **9**, the reduced product **10** is occasionally formed in the palladium-catalyzed cross-coupling reaction of **5** with tetramethyltin using conditions reported by Echavarren and Stille.[8] In the transformation of **5** to **10**, the required hydride is probably donated intermolecularly by a palladium-catalyzed β-hydride elimination reaction of the tertiary amino group.[9,10] However, compound **9** could be formed exclusively by using conditions recently published by Saá et al.[11] These conditions were also used for the transformation of **6** to **7**.

**X-ray Crystallography.** X-ray crystallography of **3**·HCl established the presence of two independent

* Author for correspondence: Dr. Anette M. Johansson. Phone: +46-18-174336. FAX: +46-18-174024.
† Uppsala University.
‡ VTT Chemical Technology.
§ University of Arizona.
∥ Department of Pharmacology, University of Göteborg.
⊥ CNS Preclinical R&D, Astra Arcus.
▽ Department of Structural Chemistry, University of Göteborg.
⊗ Abstract published in *Advance ACS Abstracts*, January 15, 1995.

0022-2623/95/1838-0647$09.00/0 

**Scheme 1**[a]

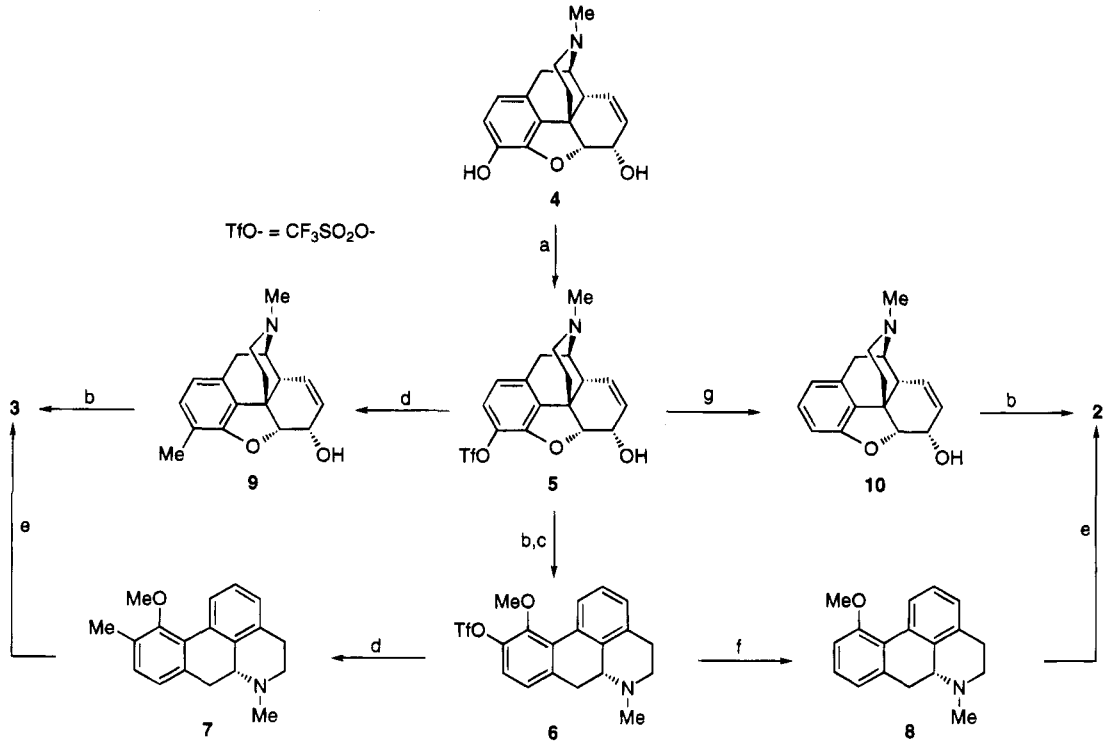


[a] Reagents: (a) $(CF_3SO_2)_2NPh$, $Et_3N$, $CH_2Cl_2$; (b) $MeSO_3H$, $N_2$, 95 °C; (c) $CH_2N_2$, $CHCl_3$, $Et_2O$; (d) $Me_4Sn$, $(PPh_3)_2PdCl_2$, $PPh_3$, LiCl, DMF, 120 °C; (e) 48% HBr (aq), $N_2$, 120 °C; (f) $Et_3N$, $HCO_2H$, $Pd(OAc)_2$, dppf, DMF, $N_2$, 60 °C; (g) $Bu_3N$, $HCO_2H$, $(PPh_3)_2PdCl_2$, dppp, DMF, $N_2$, 80 °C.

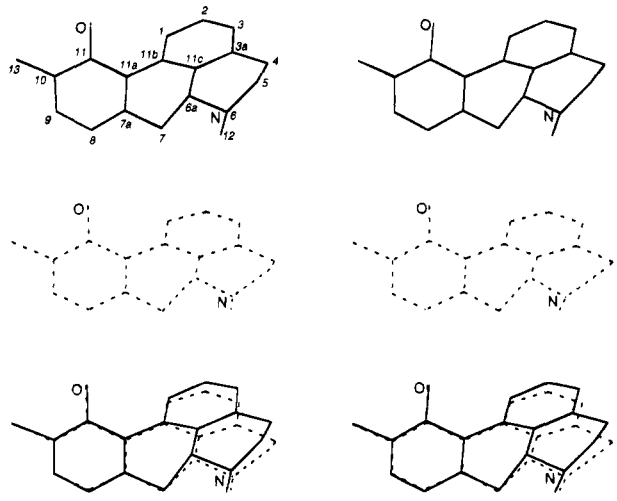

**Figure 1.** Stereorepresentation of the molecular conformation and the atomic labeling scheme for the A (top, solid lines) and B (middle, dashed lines) molecules of **3**·HCl. A best fit (bottom) between the aromatic carbons of molecules A (solid lines) and B (dashed lines) of **3**·HCl is shown.

**Table 1.** Crystal Data of **3**·HCl

| | |
|---|---|
| formula | $C_{18}H_{19}NO$·HCl |
| space group | $P2_12_12_1$ |
| $a$, Å | 7.7710(10) |
| $b$, Å | 19.2708(16) |
| $c$, Å | 20.2634(36) |
| $Z$ | 8 |
| $V$, Å$^3$ | 3034.5 |
| $d_{calcd}$, g cm$^{-3}$ | 1.321 |
| $\mu$, cm$^{-1}$ | 22.2 |

conformations, A and B, in the crystal (see Figure 1, Table 1 and the Experimental Section). The two conformations are similar and differ mainly with respect to the conformation of the nonaromatic rings (see Figure 1). The conformations found in the crystal of **3**·HCl correspond to the two solid state conformations of (*R*)-apomorphine hydrochloride hydrate reported by Giesecke.[12]

**Molecular Mechanics, Semiempirical AM1, and ab Initio Calculations.** The conformational distribution of nonprotonated **1**–**3** was studied by molecular mechanics MM2(87) and MM2(91) calculations. Semiempirical AM1 and ab initio calculations at the RHF/3-21G level were performed on selected conformations of **1**–**3** in their protonated form.

Molecular mechanics calculations were essentially done as published before, except that also the aromatic hydroxylic group(s) were taken into account.[13] The preferred conformations of the aromatic hydroxylic group(s) were identified by using the torsion angle driver procedure. The results show that all three compounds have the same conformational distribution. The most stable conformation (see Figure 2) adopts a half-chair conformation of the tetrahydropyridine ring having P-helicity[14] and a pseudoequatorial *N*-methyl substituent. In this conformation the phenolic hydrogen(s) is located above the C ring [$\tau_1$(C10,C11,O,O-*H*) ≈ 165° in **1**–**3** and $\tau_2$(C9,C10,O,O-*H*) ≈ 180° in **1**; Table 2]. The conformation of the phenolic hydrogen(s) having $\tau_1$ and $\tau_2$ = 0° has a relative steric energy ($\Delta E_s$) around 2.5 kcal/mol.

Semiempirical (AM1) calculations were performed on the protonated form of low-energy MM2 conformations of **1**–**3**. The lowest energy conformers of **1**–**3** generated by AM1 are almost identical to the MM2 conformations of lowest energy. The only deviation observed was the conformation of the hydroxyl group(s) which has $\tau_1$ and $\tau_2$ values around 0° according to the AM1 calculations (Table 2). The corresponding AM1 conformations, with

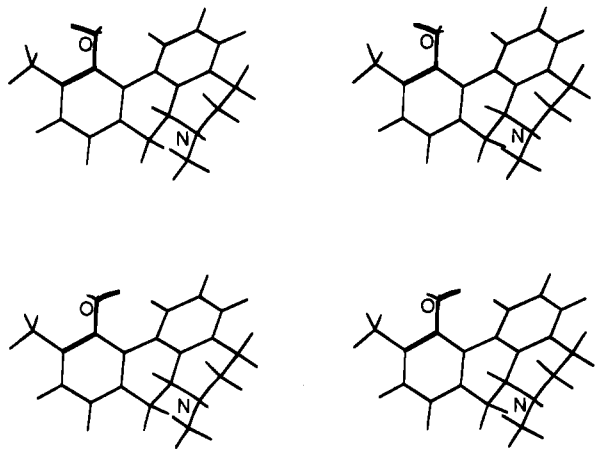

**Figure 2.** Stereorepresentation of low-energy conformations of **3** generated by MM2(91) having $\tau_1 = 0°$ (top) and 180° (bottom).

**Table 2.** Low-Energy Conformations of **2** and **3** Generated by MM2(91) and of Protonated **2** and **3** Generated by AM1 and ab Initio Calculations at the RHF/3-21G Level

| method | conformation | $\tau_1$(C10,C11,O,O-*H*) (deg) | $\Delta E_s$ (kcal/mol) |
|---|---|---|---|
| MM2(91) | | | |
| | **2a** | 7.1 | 2.3 |
| | **3a** | 8.5 | 2.7 |
| | **2b** | 165 | 0 |
| | **3b** | 165 | 0 |
| AM1 | | | |
| | **2a** | 2.2 | 0 |
| | **3a** | 4.2 | 0 |
| | **2b** | 153 | 2.0 |
| | **3b** | 152 | 2.2 |
| RHF/3-21G | | | |
| | **2a** | 5.5 | 0 |
| | **3a** | 12 | 0 |
| | **2b** | 129 | 2.3 |
| | **3b** | 130 | 1.1 |

$\tau_1$ around 140−150° and $\tau_2$ around 180°, have $\Delta E_s \approx$ 2.0 kcal/mol.

Ab initio calculations at the RHF/3-21G level were performed on the lowest energy AM1 conformations of **2** and **3** with the two different conformations of the hydroxylic group. The results show that the lowest energy conformations of the hydroxyl group have $\tau_1$ around 0° and the other conformation, having $\tau_1$ around 130°, is 1−2 kcal/mol higher in energy.

In contrast to AM1 and ab initio calculations, the lowest energy MM2(91) conformations of **1**−**3** have the C11-phenolic hydrogen located above the aromatic C ring. These MM2(91) conformations are stabilized by van der Waals interactions between the C11-phenolic hydrogen and the carbon atoms of the aromatic C ring (C1, C2, C3, C3a, C11b, and C11c). Recently, results were reported by Jansen et al.[15] and Wikström et al.[16] where stabilizing van der Waals interactions between an amide hydrogen or an ammonium hydrogen and the carbon atoms of an aromatic ring were obtained with MM2(85). Apparently, these electrostatic interactions between the phenolic hydrogen and the aromatic ring are less important according to AM1 and ab initio calculations at the RHF/3-21G level.

**Receptor Modeling.** A model of a human 5-$HT_{1A}$ receptor[17] was constructed according to a strategy previously described for modeling of the muscarinic m1 receptor[18] and the dopamine $D_{2A}$ and $D_3$ receptors.[19] In short, the models are based on a presumed homology in three-dimensional structure between bacteriorhodopsin and the G-protein-coupled (GPC) receptors. α-Helices were constructed from the amino acid sequence of the human 5-$HT_{1A}$ receptor.[20] Transmembrane regions were determined by examining hydropathy plots and multiple sequence alignments of a number of GPC receptors. The relative rotations of the helices were estimated by considering conserved amino acids and hydropathy moment plots. The α-helices ($\phi = -55.02$ and $\psi = -50.43$) were constructed from the amino acid sequences of the TMs, and proline kinks were taken into account. Side chain conformations from rotamer libraries were used. The helices were energy minimized using AMBER all atom force field. Fitting of the backbone of these helices onto the backbone of bacteriorhodopsin produced the TM bundle of the receptors. The loop regions were not included in the modeling. The side chains were adjusted manually to avoid overlap produced by the fitting procedure. The resulting TM bundle was energy minimized (AMBER united-atom force field—2000 iterations and AMBER all-atom force field—500 iterations) with no restrictions of the backbone. Similar models of the 5-$HT_{1A}$ receptor have recently been reported by others.[21]

A common binding site for agonists at the 5-$HT_{1A}$ receptor was probed by using the receptor-excluded volume derived from the indirect model of potent 5-$HT_{1A}$ receptor agonists developed by Mellin et al.[22] The receptor-excluded volume produced by the indirect model was well accommodated by the 5-$HT_{1A}$ binding-site.[23] Further, the model is in agreement with results from site-directed mutagenesis studies which indicate that (a) the aspartate residues Asp82 (TM2) and Asp116 (TM3) are of importance for the binding of agonists.[24] Asp116 is probably the primary binding site for endogenous ligands having a protonated nitrogen in analogy with many other GPC receptors.[25] Asp82 may have an allosteric effect on agonist affinity in accordance with the $D_2$ and $\alpha_2$ receptors where the corresponding residue has been mutated. This resulted in an impaired sodium effect when binding agonists.[26] (b) The serine residue Ser198 (TM5) is of importance for agonist binding to the 5-$HT_{1A}$ receptor since a mutation of Ser198 (TM5) to Ala198 reduced the affinity of 5-HT 100-fold.[24b] This is in analogy with the $D_2$ receptor, where a mutation of the corresponding residue (Ser193) reduced the affinity of agonist ligands.[27]

Low-energy conformations of **1**−**3** were manually fitted into the binding-site models of the 5-$HT_{1A}$ receptor and the $D_{2A}$ receptor. During the fitting procedure, repulsive interactions were minimized and attractive interactions were optimized.

## Pharmacology

Compounds **2** and **3** were examined *in vitro* for their ability to displace [$^3$H]-8-OH-DPAT, [$^3$H]SCH23390, and [$^3$H]raclopride binding to rat hippocampal 5-$HT_{1A}$, rat striatal $D_1$, and cloned human $D_{2A}$ receptors, respectively (Table 3). In Table 3 the affinities of (*R*)-apomorphine (**1**) for these receptors are also included. Several $D_1$ and $D_{2A}$ receptor agonists display high- and low-affinity binding-sites in *in vitro* receptor binding assays using antagonists as ligands.[19,28] However, in the present investigation none of the compounds test-

**Table 3.** Affinities of **1**–**3** for Rat Brain 5-$HT_{1A}$ and $D_1$ Receptor Recognition Sites Labeled by [$^3$H]-8-OH-DPAT and [$^3$H]SCH23390, Respectively, and at Cloned Human $D_{2A}$ Receptors Expressed in Ltk$^-$ Cells and Labeled by [$^3$H]Raclopride

| | $K_i$ (nM) | | |
|---|---|---|---|
| compd | [$^3$H]-8-OH-DPAT (5-$HT_{1A}$) | [$^3$H]SCH23390 ($D_1$) | [$^3$H]raclopride ($D_{2A}$) |
| **1** | 296 ± 15 | 236[a] | 41.9 ± 4.7 |
| **2** | 9.6 ± 3.1 | 20.4 ± 1.0 | 58.5 ± 9.5 |
| **3** | 0.45 ± 0.13 | 382 ± 35 | 1070 ± 54 |

[a] From ref 2b.

**Table 4.** Inhibition of 5-HT-Sensitive, Forskolin-Stimulated Adenylyl Cyclase *in Vitro*

| compd | potency, $EC_{50}$ (nM)[a] | maximal inhibition (%)[b] | $EC_{50}$ (nM)/$K_i$ (5-$HT_{1A}$; nM)[c] |
|---|---|---|---|
| **2** | 5200 | 60 | 542 |
| **3** | 55 | 102 | 122 |

[a] $EC_{50}$ values represent the mean of three determinations in the FSC assay, as calculated by nonlinear regression analysis. [b] Percentage of inhibition of the 5-HT-sensitive component of FSC. [c] See Table 3.

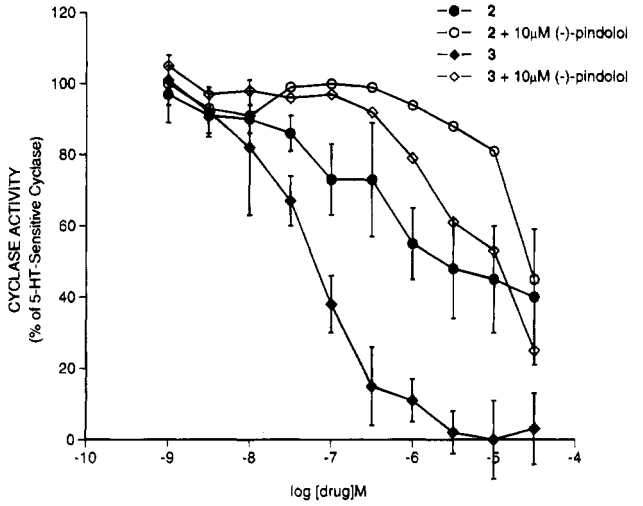


**Figure 3.** Effects of **2** (●) and **3** (◆) on FSC activity alone and in the presence of 10 μM (−)-pindolol (○ and ◇, respectively). Cyclase activity is expressed as the percent of 5-HT-sensitive forskolin-stimulated adenylyl cyclase activity in the rat hippocampal membranes, and each point represents the mean ± SEM. The number of individual experiments for each dose–response curve is three, and all points are the mean ± standard error.

ed produced a clear biphasic binding profile at the $D_1$ and/or $D_{2A}$ receptor. Therefore, the results have been interpreted in terms of a one-site model. The results show that **3** has high affinity and selectivity for 5-$HT_{1A}$ receptors, while **2** is nonselective with moderate affinity for the receptors studied. In comparison, **1** selectively binds to $D_{2A}$ receptors.

The ability of the compounds to inhibit forskolin-stimulated adenylyl cyclase (FSC) activity in rat hippocampal membranes *in vitro* was also studied. Since the inhibition of FSC activity in hippocampal membranes is believed to be mediated through 5-$HT_{1A}$ receptors,[29] this assay discriminates between 5-$HT_{1A}$ receptor agonists and antagonists. The results in Table 4 and Figure 3 show that **3** acts as a full agonist, i.e., it inhibits cyclase activity to the same degree as 5-HT. The FSC inhibition caused by **3** was fully antagonized by (−)-pindolol, a nonselective 5-$HT_{1A}$ receptor antagonist,

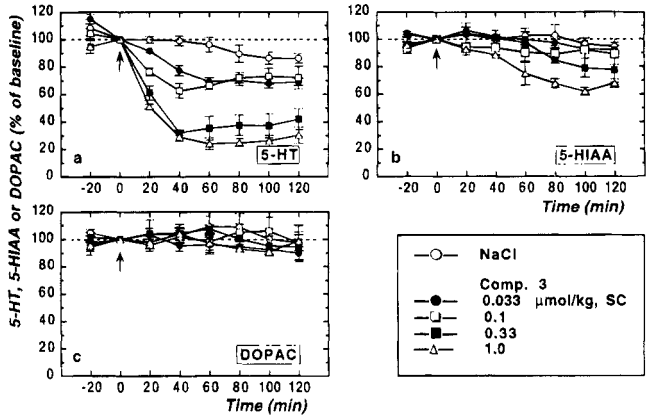


**Figure 4.** Effects of **3** on rat ventral hippocampal output of 5-HT (a), 5-HIAA (b), and DOPAC (c) *in vivo*. Rats were given NaCl (○) or compound **3** [0.033 (●), 0.1 (□), 0.33 (■), or 1.0 (△) μmol/kg sc]. The dialysate contents of 5-HT, 5-HIAA, and DOPAC were determined for 2 h after drug or vehicle injection (arrow). Data represent means ± SEM ($n$ = 3–5) and are expressed as a percentage of the corresponding preinjection base-line dialysate levels. The overall output of 5-HT and 5-HIAA 0–120 min after injection (AUC) was significantly ($p \leq 0.01$) suppressed vs NaCl controls by **3** (doses ≥ 0.03 and 0.3 μmol/kg sc, respectively). Dashed line depicts 100% predrug base-line level.

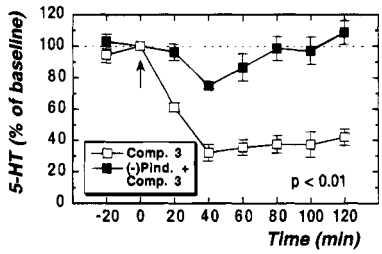


**Figure 5.** Antagonism of the induced reduction of 5-HT release by means of the 5-$HT_{1A}$ receptor blocker (−)-pindolol. Compound **3** (0.3 μmol/kg sc) was given to untreated (□; data from Figure 4) or (−)-pindolol-treated (■; 32 μmol/kg sc, 40 min prior to **3**) rats. Dialysates were collected every 20 min and analyzed for 5-HT for 2 h thereafter. Shown are the means ± SEM ($n$ = 4–5), expressed as a percentage of the corresponding absolute base-line values of 5-HT. The overall 5-HT output-suppressing response 0–120 min (AUC) to compound **3** was significantly antagonized by systemic ($P$ = 0.05) treatment. Dashed line depicts 100% preagonist level (from Figure 4.).

which is consistent with the effect occuring via 5-$HT_{1A}$ receptor stimulation. Compound **2**, on the other hand, was shown to be a partial agonist. It inhibited FSC to about 60% of the maximal effect produced by 5-HT.

The *in vivo* effects of **2** and **3** on rat hippocampal output of 5-HT, 5-hydroxyindoleacetic acid (5-HIAA), and dihydroxyphenylacetic acid (DOPAC) were studied using *in vivo* microdialysis. The dialysate levels of 5-HT, 5-HIAA, and DOPAC were taken as indices of 5-HT release and metabolism/turnover and catecholamine [mainly norepinephrine (NA)] metabolism/turnover, respectively.[30] Compound **3** induced a dose- and time-dependent suppresion of the rat ventral hippocampal 5-HT release (Figure 4a). The approximate $ID_{50}$ for this response, estimated from area under the curve (AUC) data, was 0.1 μmol/kg. The 5-HT release-suppressing action of **3** (0.3 μmol/kg) was antagonized by (−)-pindolol (Figure 5). Also the 5-HIAA output was reduced in a dose-dependent manner by **3**; significant

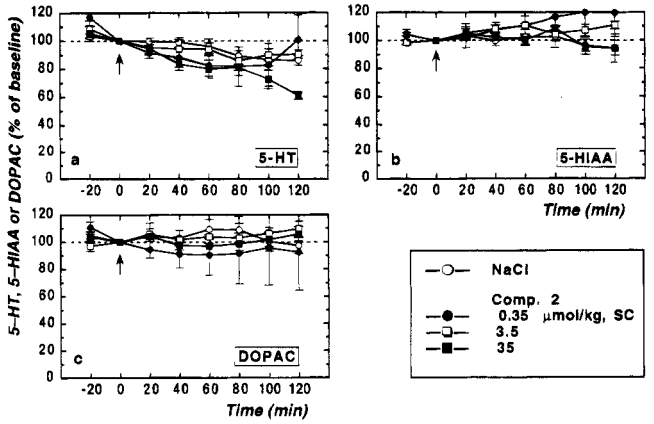


**Figure 6.** Effects of **2** on rat ventral hippocampal output of 5-HT (a), 5-HIAA (b), and DOPAC (c) *in vivo*. Rats were given NaCl (○) or compound **2** [0.35 (●), 3.5 (□), and 35 (■) μmol/kg sc]. The dialysate contents of 5-HT, 5-HIAA, and DOPAC were determined for 2 h after drug or vehicle injection (arrow). Data represent means ± SEM ($n$ = 3–5) and are expressed as a percentage of the corresponding preinjection base-line dialysate levels. The overall output of 5-HT, 5-HIAA, and DOPAC 0–120 min after injection (AUC) was not significantly altered vs NaCl controls by **2**. Dashed line depicts 100% predrug base-line level.

($p \leq 0.05$) effects in this respect were obtained after the two highest doses of the compound (Figure 4b).

In contrast to **3**, compound **2** (0.35–35.0 μmol/kg sc) failed to significantly alter the overall dialysate output of 5-HT (Figure 6a); a weak decrease was noted after the highest dose only. Moreover, in preliminary studies ($n$ = 2; data not shown), **2** (35 μmol/kg sc) failed to appreciably affect the 5-HT release-reducing response by the 5-$HT_{1A}$ autoreceptor agonist **11** (8-OH-DPAT, 0.09 μmol/kg sc). The dialysate concentrations of 5-HIAA were not significantly altered by **2** (Figure 6b). Neither **2** nor **3** produced consistent effects on the DOPAC output levels Figures 4c and 6c).

## Discussion

The present data are consistent with the characterization of **3** as a potent, efficacious, and selective 5-$HT_{1A}$ receptor agonist. Thus, **3** displayed high selectivity and affinity for 5-$HT_{1A}$ receptors, and in the FSC assay, **3** appeared to be a full agonist by inhibiting about 100% of the activity of the 5-HT-sensitive adenylyl cyclase. In addition, **3** dose-dependently suppressed the ventral hippocampal dialysate output of 5-HT and 5-HIAA *in vivo*, indicating decreased 5-HT release and metabolism/turnover, respectively. The two latter responses were inhibited by the 5-$HT_{1A}$ antagonist (−)-pindolol, indicating involvement of 5-$HT_{1A}$ receptors. The responses elicited by **3** in these tests are comparable in potency and apparent efficacy to those previously obtained with the selective 5-$HT_{1A}$ receptor agonist (*R*)-**11**.[30b,31]

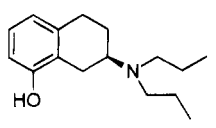


(*R*)-11

Compound **2** at best weakly reduced the output of 5-HT in doses up to 35 μmol/kg sc (Figure 6a). Further, **2** was only able to inhibit about 60% of 5-HT-sensitive adenylyl cyclase activity, and this inhibition was (−)-pindolol sensitive. In addition, **2** was shown to have moderate affinity for central 5-$HT_{1A}$ receptors. These results indicate that **2** acts as a weak partial agonist on 5-$HT_{1A}$ receptors.

DOPAC is one of the major DA metabolites. However, the DA innervation to the NA-predominated hippocampus is very scarce, and the DOPAC found in dialysates from this area is more likely to reflect the metabolism of DA formed in NA neurones.[30c] The lack of significant effects of **2** and **3** on the dialysate DOPAC levels may therefore tentatively suggest a lack of potent $\alpha_2$-adrenoceptor agonist activity, whereas any conclusion as to the DA potential of these compounds has to await further studies.

The pronounced difference in pharmacology between **1**, **2**, and **3** is demonstrated by the receptor binding data: whereas **1** has a preference for $D_{2A}$ receptors (Table 3),[2b] **3** is selective for 5-$HT_{1A}$ receptors and **2** is nonselective. The above findings, together with previously published results,[5] show that **3** is a potent, efficacious, and selective 5-$HT_{1A}$ receptor agonist. In contrast, **2** appears to be a weak partial agonist at 5-$HT_{1A}$ receptors.

To be able to rationalize the different pharmacological profiles of **1**–**3**, we docked the lowest energy conformations of the ligands into the binding-site of homology-derived receptor models of the $D_{2A}$ and 5-$HT_{1A}$ receptors. According to these modeling studies, the aporphines can interact with the $D_{2A}$ receptor in a similar way as the 2-aminotetralin derivatives[19] and the neurotransmitter dopamine.[21a] A reinforced electrostatic attraction between the protonated nitrogen of the ligands and the carboxylate of Asp114 in TM3 anchors the ligand to the receptor. A hydrogen bond can be formed between Ser193 in TM5 and the phenolic hydrogen at C11 in the three ligands. In addition, an aromatic edge to face interaction between the aromatic A ring of **1**–**3** and Phe390 in TM6 is present (Figure 7).

In the binding-site model of the 5-$HT_{1A}$ receptor, one serine residue is available (Ser198, TM5) for hydrogen bonding with the C11-phenolic hydrogen in aporphines **1**–**3**. A reinforced electrostatic interaction between the cationic nitrogen of the ligands and the carboxylate of Asp116 in TM3 and an aromatic interaction between the A ring of the ligands and the phenyl ring in Phe361 in TM6 are also present (Figure 7).

The dockings of **1**–**3** into the binding-site model of the $D_{2A}$ receptor show that **1** and **2** fit well into the binding-site. Both **1** and **2** donate a hydrogen bond from their C11-hydroxyl group to Ser193 in TM5. In **1** the C10-hydroxyl group may accept an intramolecular hydrogen bond from the C11-hydroxyl group.

Introduction of a methyl group at C10 in the aporphine skeleton, giving **3**, decreases the affinity for $D_{2A}$ receptors dramatically. This decrease in affinity appears to be due to a steric repulsion between the C10-methyl group and the binding site of the $D_{2A}$ receptor (Figure 8).

When docking aporphines **1**–**3** into the binding-site of the 5-$HT_{1A}$ receptor, **3** produced a better fit than **1** and **2**. Examination of the interaction between **3** and the 5-$HT_{1A}$ binding-site model revealed that the C10-methyl group fits into a lipophilic cavity, which is large enough to accommodate a methyl group (Figure 9). This interaction may increase the total van der Waals

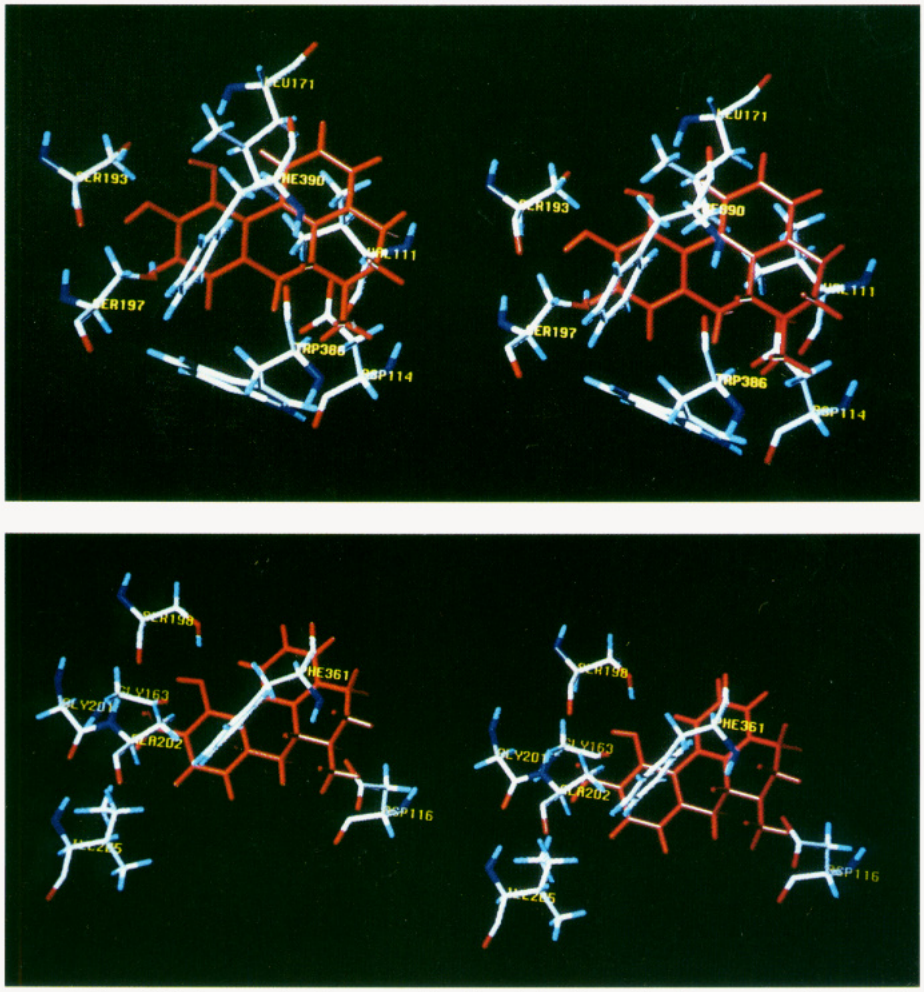


**Figure 7.** Stereorepresentation of the interaction between **1** (red) and the dopamine $D_2$ receptor binding site model (top) and the interaction between **3** (red) and the 5-$HT_{1A}$ receptor binding site model (bottom).

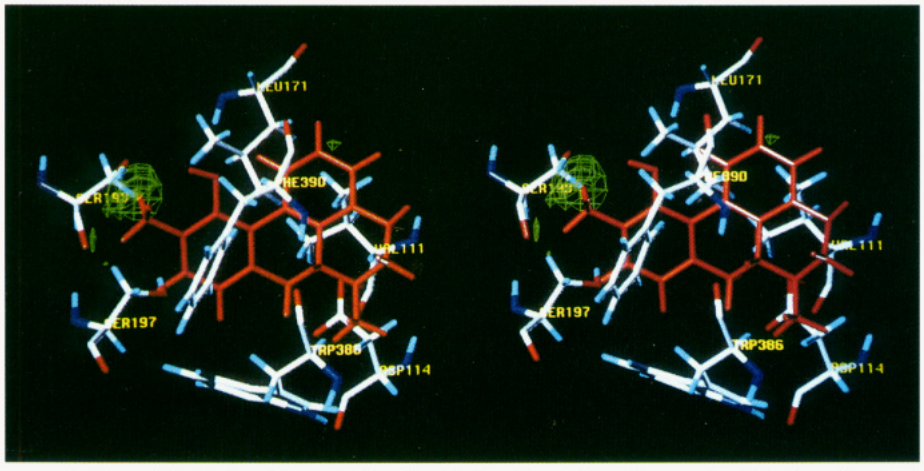


**Figure 8.** Stereorepresentation of the interaction of **3** (red) with the dopamine $D_2$ receptor binding site model. The unfavorable interaction between the C10-methyl group of **3** and the binding site model is shown in green.

contribution to the binding between **3** and the 5-$HT_{1A}$ receptor and would thus explain the surprisingly high affinity of **3** for 5-$HT_{1A}$ receptors.

The low affinity of **1** for 5-$HT_{1A}$ receptors may be explained by comparing the docking of **1** into the 5-$HT_{1A}$ binding-site model with that of **3**. When **1** interacts with the 5-$HT_{1A}$ binding-site model, in the same manner as **3**, an electrostatic repulsion is present between the closely situated C10-hydroxyl group of **1** and the carbonyl group of Gly163 in TM5 (Figure 10). This electrostatic repulsion may make the interaction of **1** with the 5-$HT_{1A}$ binding-site unfavorable.

Compound **2** fits well into the 5-$HT_{1A}$ binding-site model. However, the absence of a group in the C10-position, which would increase the total van der Waals contribution, may explain the decreased affinity of **2** for 5-$HT_{1A}$ receptors.

In summary, the results indicate that **3** is a potent, selective, and efficacious 5-$HT_{1A}$ receptor agonist. In contrast, **2** is a partial 5-$HT_{1A}$ receptor agonist of low

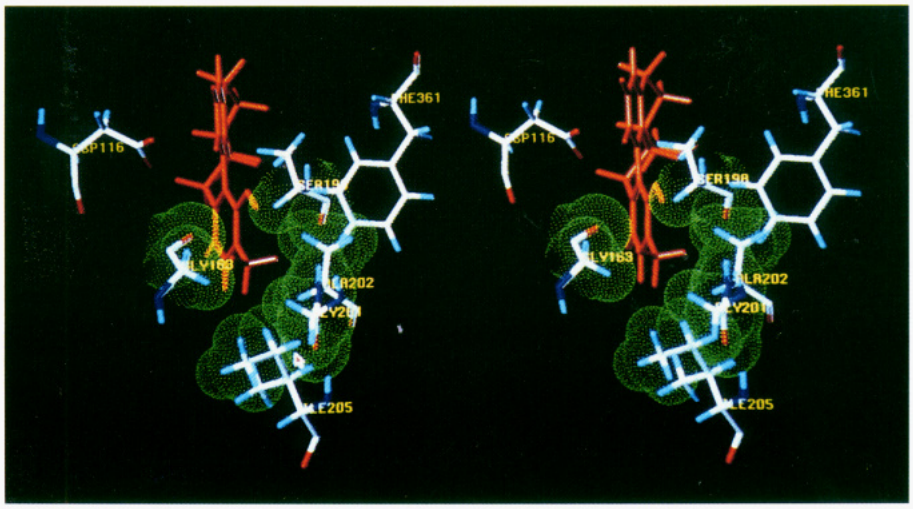


**Figure 9.** Stereorepresentation of the interaction of the C10-methyl group of **3** (red) with the 5-$HT_{1A}$ receptor binding site model. The methyl group fits into a cavity defined by Ala202, Ile205, Gly201, Ser198, and Gly163 and shown by a green van der Waals dot surface.

potency which has affinity also for central $D_1$ and $D_{2A}$ receptors. The selective and pronounced serotonergic effects of **3** can be rationalized by the 5-$HT_{1A}$ binding-site model in which the C10-methyl group is accommodated by a lipophilic pocket, which is not present in the $D_{2A}$ binding-site.

## Experimental Section

**Chemistry. General Comments.** Melting points (uncorrected) were determined in open glass capillaries on an Electrothermal melting point apparatus. Optical rotation measurements were obtained on a Perkin-Elmer 241 polarimeter. Elemental analyses (C, H, N) were performed at Mikrokemi AB, Uppsala, Sweden, and determined within 0.4% of the theoretical values. $^1$H- and $^{13}$C-NMR spectra were recorded on a JEOL JNM-EX270 spectrometer at 270 and 67.5 MHz, respectively, and referenced to internal tetramethylsilane. $^{19}$F-NMR and some $^{13}$C-NMR spectra were recorded at 84.5 and 15 MHz, respectively, using a JEOL FX-90Q spectrometer and referenced to internal $CFCl_3$ ($^{19}$F) and tetramethylsilane ($^{13}$C). Infrared (IR) spectra were recorded on a Perkin-Elmer 298 infrared spectrophotometer. Thin-layer chromatography (TLC) was performed by using aluminum sheets precoated with either silica gel 60 $F_{254}$ or aluminum oxide 60 $F_{254}$ E neutral (0.2 mm; E. Merck). For preparative TLC, plates precoated with either silica gel 60 $F_{254}$ (2.0 mm) or aluminum oxide $F_{254}$ T (1.5 mm) (E. Merck) were used. Column chromatography was performed on silica gel 60 (230–400 mesh; E. Merck) or aluminum oxide 90 (70–230 mesh; E. Merck).

**(−)-3-*O*-[(Trifluoromethyl)sulfonyl]morphine (5). Method A.** A slurry of **4**·$H_2O$ (2.79 g, 9.20 mmol) and $Et_3N$ (1.92 mL, 13.8 mmol) in $CH_2Cl_2$ (150 mL) kept under nitrogen was stirred for 1 h at room temperature. *N*-Phenyltrifluoromethanesulfonimide (3.94 g, 11.0 mmol) was added, and after being stirred for 48 h, the reaction mixture was extracted with 10% aqueous $NaHCO_3$. The organic layer was dried ($K_2CO_3$), filtered, and concentrated *in vacuo*. The oily residue was chromatographed [$SiO_2$; $CHCl_3$–MeOH (gradient 39:1–9:1)]. Three recrystallizations of the amine from ether gave 3.45 g (90%) of pure **5**: mp 123–124 °C; $[\alpha]^{21}_D$ −77.8° (*c* 1.0, MeOH); IR (KBr) 3550 $cm^{-1}$ ($\nu$ OH); $^1$H NMR[32] ($CDCl_3$) $\delta$ 1.89 (1 H, ddd, $J_{15eq,15ax}$ = 12.6 Hz, $J_{15eq,16ax}$ = 3.6 Hz, $J_{15eq,16eq}$ = 1.7 Hz, H-15eq), 2.10 (1 H, ddd, $J_{15ax,16ax}$ = 12.3 Hz, $J_{15ax,16eq}$ = 5.0 Hz, H-15ax), 2.31 (1 H, dd, $J_{10ax,9}$ = 6.1 Hz, $J_{10ax,10eq}$ = 19.0 Hz, H-10ax), 2.34 (1 H, ddd, H-16ax), 2.44 (3 H, s, N-$CH_3$), 2.61 (1 H, ddd, $J_{16eq,16ax}$ = 12.2 Hz, H-16eq), 2.69–2.71 (1 H, m, H-14), 2.80 (1 H, br s, OH), 3.09 (1 H, app d, H-10eq), 3.37 (1 H, dd, $J_{9,14}$ = 3.3 Hz, H-9), 4.19–4.23 (1 H, m, H-6), 5.01 (1 H, dd, $J_{5,6}$ = 6.3 Hz, $J_{5,7}$ = 1.2 Hz, H-5), 5.28 (1 H, ddd, $J_{8,6}$ = 3.3 Hz, $J_{8,7}$ = 9.9 Hz, $J_{8,14}$ = 2.1 Hz, H-8), 5.67–5.73 (1 H, m, H-7), 6.63 (1 H, app d, $J_{1,2}$ = 8.6 Hz, H-1), 6.89 (1 H, d, H-2); $^{13}$C NMR[33] ($CDCl_3$) $\delta$ 20.9 (C-10), 35.2 (C-15), 40.5 (C-14), 43.0 (N-$CH_3$), 43.3 (C-13), 46.0 (C-16), 58.5 (C-9), 66.5 (C-6), 93.6 (C-5), 118.7 (q, $J_{C,F}$ = 321 Hz, $CF_3$), 120.0 (C-1), 121.0 (C-2), 128.3 (C-8), 130.6 (C-12), 133.6 (C-7), 133.8 (C-11), 135.7 (C-3), 149.5

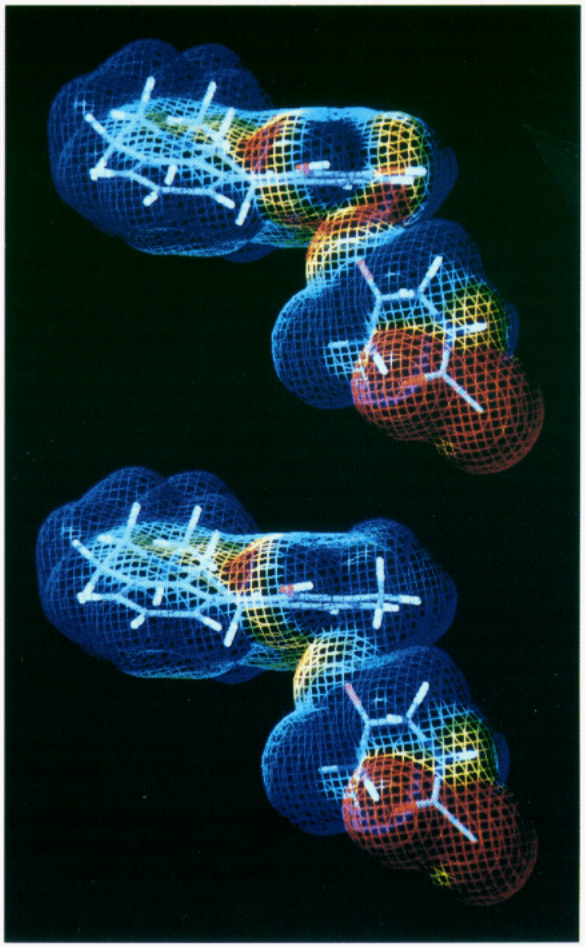

**Figure 10.** Electrostatic interactions between Gly163 in the 5-$HT_{1A}$ receptor binding site and **1** (top) and **3** (bottom). For clarity, the range of electrostatic potential displayed on the electron density surface is restricted to a range from 20.0 to 60.0 kcal/mol. Red represents the lowest and blue the highest electrostatic potential.

(C-4); $^{19}$F NMR ($CDCl_3$) $\delta$ −73.9 (s, $CF_3$). Anal. ($C_{18}H_{18}F_3NO_5S$) C, H, N.

**Method B.** A slurry of **4**·HCl·$(H_2O)_3$ (4.36 g, 11.6 mmol), $Et_3N$ (4.84 mL, 34.8 mL), and $CH_2Cl_2$ (200 mL) kept under nitrogen was stirred for 1 h at room temperature. *N*-Phenyltrifluoromethanesulfonimide (6.22 g, 17.4 mmol) was added, and the mixture was stirred under reflux for 2 h and then at room temperature for 40 h. Workup as in method A gave 3.89 g (82%) of pure **5**.

**(−)-(*R*)-11-Methoxy-10-[[(trifluoromethyl)sulfonyl]oxy]-aporphine (6).** A solution of **5** (2.78 g, 6.66 mmol) in concentrated $MeSO_3H$ (12 mL) was kept under nitrogen at 95 °C for 1.5 h. The reaction mixture was partitioned between $CHCl_3$ (200 mL) and 10% aqueous $NaHCO_3$ (150 mL). The aqueous phase was extracted with $CHCl_3$ (3 × 150 mL), and the combined organic layers were dried ($Na_2SO_4$) and filtered. An etheral solution of $CH_2N_2$, generated from *p*-tolylsulfonylmethylnitrosamide (14.3 g, 66.7 mmol), was added to the stirred chloroform solution at room temperature. Excess $CH_2N_2$ was destroyed after 3 h by addition of glacial HOAc. The mixture was extracted with 10% aqueous $NaHCO_3$ (300 mL), dried ($K_2CO_3$), filtered, and concentrated *in vacuo* to give 3.04 g of **6** as a yellow oil. A second batch of **6** starting from **5** (2.70 g, 64.7 mmol) was prepared. The two batches were combined, and the crude oil was purified by flash chromatography [$Al_2O_3$; ether/hexane (1:1)]. The amine was converted into the hydrochloride giving 4.50 g of **6**·HCl (76%): mp 207−209 °C dec; $[\alpha]^{21}_D$ −48.0° (*c* 1.0, MeOH); IR (KBr) 1220, 1140 cm$^{-1}$ ($\nu$ S=O stretch); $^1$H NMR ($CD_3OD$) $\delta$ 2.93 (1 H, app t, $J_{7\alpha,7\beta} = J_{7\alpha,6a\beta}$ = 14 Hz, H-7$\alpha$), 3.10−3.20 (1 H, m, H-4), 3.19 (3 H, s, N-C$H_3$), 3.41−3.68 (3 H, m, H-4, H-5, H-7$\beta$), 3.68 (s, O-C$H_3$), 3.81−3.88 (1 H, m, H-5), 4.51 (1 H, dd, $J_{6a\beta,7\beta}$ = 2 Hz, H-6a$\beta$), 7.33 (1 H, app d, H-3), 7.33 (2 H, app s, H-8, H-9), 7.44 (1 H, dd, $J_{1,2}$ = 7.9 Hz, $J_{2,3}$ = 7.6 Hz, H-2), 8.25 (1 H, app d, H-1); $^{13}$C NMR ($CD_3OD$) $\delta$ 26.8 (C-4), 32.4 (C-7), 41.9 (N-*C*$H_3$), 53.4 (C-5), 61.7 (O-*C*$H_3$), 62.7 (C-6a), 120.1 (q, $J_{C,F}$ = 320 Hz, $CF_3$), 122.9 (C-8), 126.3, 127.9, 129.5, 130.1, 130.4, 130.6, 131.4, 131.5, 136.5, 144.6, 151.2 (C-11); $^{19}$F NMR ($CD_3OD$) $\delta$ −74.3 (s, $CF_3$). Anal. ($C_{19}H_{20}ClF_3NO_4S$) C, H, N.

**(−)-(*R*)-11-Methoxy-10-methylaporphine (7).** Compound **7** was prepared from **6** according to a method previously described by Saá et al.[11] A solution of **6** (500 mg, 1.2 mmol) in dry DMF (3 mL) was added to a mixture of $(PPh_3)_2PdCl_2$ (100 mg, 0.14 mmol), LiCl (420 mg, 9.9 mmol), and $PPh_3$ (190 mg, 0.72 mmol) in 7 mL of dry DMF. After the mixture had stirred for 2 min at room temperature, $(CH_3)_4Sn$ (0.67 mL, 4.8 mmol) and three crystals of 2,6-di-*tert*-butyl-4-methylphenol were added. The flask was carefully sealed, and the reaction mixture was stirred at 120 °C for 19 h. The volatiles were evaporated *in vacuo*, and the residue was partitioned between $CHCl_3$ and 10% aqueous $NaHCO_3$. The combined organic extracts were washed with 10% aqueous KF, dried ($K_2CO_3$), filtered, and concentrated to give a brown oil. Column chromatography [$SiO_2$; $CHCl_3$/MeOH (39:1); and $Al_2O_3$; ether/hexanes (1:1)] gave the amine as a colorless oil. The pure amine was converted into the hydrochloride salt which was recrystallized from $CH_3CN$−ether providing 292 mg (77%) of pure **7**·HCl: mp 189−191 °C; $[\alpha]^{21}_D$ −179.0° (*c* 1.0, MeOH); IR (KBr) 2360 cm$^{-1}$ ($\nu$ $R_3NH^+$); $^1$H NMR ($CD_3OD$) $\delta$ 2.32 (3 H, s, Ar-C$H_3$), 2.85 (1 H, app t, $J_{7\alpha,7\beta} = J_{7\alpha,6a\beta}$ = 14 Hz, H-7$\alpha$), 3.11−3.20 (1 H, m, H-4), 3.18 (3 H, s, N-C$H_3$), 3.35−3.64 (3 H, m, H-4, H-5, H-7), 3.50 (3 H, s, O-C$H_3$), 3.77−3.83 (1 H, m, H-5$\alpha$), 4.41 (1 H, dd, $J_{6a\beta,7\beta}$ = 2.8 Hz, H-6a$\beta$), 7.08 (1 H, app d, $J_{8,9}$ = 8.1 Hz, H-8), 7.17 (1 H, d, H-9), 7.24 (1 H, app d, $J_{2,3}$ = 7.6 Hz, H-3), 7.40 (1 H, dd, $J_{1,2}$ = 7.9 Hz, H-2), 8.35 (1 H, app d, H-1); $^{13}$C NMR ($CD_3OD$) $\delta$ 16.4 (Ar-*C*$H_3$), 27.0 (C-4), 32.6 (C-7), 42.2 (N-*C*$H_3$), 53.4 (C-5), 60.1 (O-*C*$H_3$), 63.4 (C-6a), 125.2 (C-8), 126.8, 127.8, 129.1, 129.6, 129.8, 130.9, 132.1, 133.0, 133.2, 133.5, 157.6 (C-11). Anal. ($C_{19}H_{22}ClNO$) C, H, N.

**(−)-(*R*)-11-Methoxyaporphine (8).**[5,6,34] Compound **8** was prepared from **6** according to a method previously described by Cacchi et al.[35] A solution of $Et_3N$ (0.39 mL, 2.72 mmol) and $HCO_2H$ (69 $\mu$L, 1.8 mmol) was added to a mixture of **6** (300 mg, 0.726 mmol), $Pd(OAc)_2$ (16 mg, 0.073 mmol), and 1,1′-bis(diphenylphosphino)ferrocene (dppf) (60 mg, 0.11 mmol) in DMF (5 mL). The reaction mixture was stirred under nitrogen at 60 °C for 22 h and then partitioned between ether and water. The organic phase was washed with brine, dried ($K_2CO_3$), filtered, and concentrated *in vacuo*. The oily residue was chromatographed [$Al_2O_3$; ether followed by $SiO_2$; $CHCl_3$/MeOH (gradient 39:1−9:1)]. The resulting amine was converted into the hydrochloride affording 193 mg (87%) of pure **8**·HCl: mp 236−238 °C dec (lit.[6] mp 235−242 °C dec; lit.[5] mp 246−248 °C; lit.[34] mp 253−255 °C); $[\alpha]^{21}_D$ −98.9° (*c* 1.0, MeOH) [lit.[3] $[\alpha]^{21}_D$ −97.5° to −99.1° (*c* 1.0, MeOH); lit.[34] $[\alpha]^{21}_D$ −92.6° (*c* 0.606, MeOH)]; $^1$H NMR ($CD_3OD$) $\delta$ 2.89 (1 H, app t, $J_{7\alpha,6a\beta} = J_{7\alpha,7\beta}$ = 14 Hz, H-7$\alpha$), 3.10−3.18 (1 H, m, H-4), 3.15 (3 H, s, N-C$H_3$), 3.34−3.47 (3 H, m, H-4, H-5, H-7$\beta$), 3.71−3.79 (1 H, m, H-5), 3.88 (3 H, s, O-C$H_3$), 4.29 (1 H, dd, $J_{6a\beta,7\alpha}$ = 2.8 Hz, H-6a$\beta$), 6.99 (1 H, app d, $J_{10,9}$ = 7.5 Hz, H-10), 7.05 (1 H, app d, $J_{8,9}$ = 8.0 Hz, H-8), 7.17 (1 H, app d, $J_{2,3}$ = 7.5 Hz, H-3), 7.27 (1 H, dd, H-9), 7.34 (1 H, dd, $J_{2,1}$ = 7.8 Hz, H-2), 8.22 (1 H, app d, H-1); $^{13}$C NMR ($CD_3OD$) $\delta$ 26.5 (C-4), 33.1 (C-7), 41.4 (N-*C*$H_3$), 53.0 (C-5), 55.9 (O-*C*$H_3$), 63.2 (C-6a), 112.6 (C-10), 121.9 (C-8), 123.0, 128.5, 128.8, 129.0, 129.1, 129.2, 130.3, 133.2, 135.7, 158.2 (C-11).

**(−)-3-Deoxy-3-methylmorphine (9).** Compound **9** was synthesized from **5** (152 mg, 0.36 mmol) using the procedure described for the preparation of **7**.[11] The reaction time was 6 h. Crude **9** was purified by chromatography [$SiO_2$; $CHCl_3$/MeOH (19:1 and 39:1−9:1 gradient)]. The amine was recrystallized from ether giving 78 mg (76%) of pure **9**: mp 181−183 °C; $[\alpha]^{21}_D$ −195.0° (*c* 1.0, MeOH); IR (film) 3540 cm$^{-1}$ ($\nu$ OH); $^1$H NMR ($CDCl_3$) $\delta$ 1.85 (1 H, ddd, $J_{15eq,15ax}$ = 12.6 Hz, $J_{15eq,16ax}$ = 3.4 Hz, $J_{15eq,16eq}$ = 1.7 Hz, H-15eq), 2.05 (1 H, ddd, $J_{15ax,16ax}$ = 12.3 Hz, $J_{15ax,16eq}$ = 5.1 Hz, H-15ax), 2.17 (3 H, s, Ar-C$H_3$), 2.29 (1 H, dd, $J_{10ax,9}$ = 6.2 Hz, $J_{10ax,10eq}$ = 18.9 Hz, H-10ax), 2.40 (1 H, m, H-16ax), 2.44 (3 H, s, N-C$H_3$), 2.58 (1 H, ddd, $J_{16eq,16ax}$ = 12.1 Hz, H-16eq), 2.67 (1 H, m, H-14), 2.87 (1 H, br s, OH), 3.06 (1 H, app d, H-10eq), 3.33 (1 H, dd, $J_{9,14}$ = 3.2 Hz, H-9), 4.84 (1 H, dd, $J_{5,6}$ = 6.6 Hz, $J_{5,7}$ = 1.1 Hz, H-5), 5.29 (1 H, ddd, $J_{8,7}$ = 9.9 Hz, $J_{8,6}$ = 3.3 Hz, $J_{8,14}$ = 2.0 Hz, H-8), 5.68 (1 H, m, H-7), 6.54 (1 H, app d, $J_{1,2}$ = 7.7 Hz, H-1), 6.82 (1 H, d, H-2); $^{13}$C NMR ($CDCl_3$) $\delta$ 14.6 (Ar-*C*$H_3$), 20.8 (C-10), 35.8 (C-15), 40.9 (C-14), 42.4 (C-13), 43.1 (N-*C*$H_3$), 46.4 (C-16), 58.8 (C-9), 66.3 (C-6), 90.2 (C-5), 116.1 (C-3), 119.0 (C-1), 128.3 (C-2), 128.8, 129.7 (C-8), 132.4, 133.3 (C-7), 156.9 (C-4). Anal. ($C_{18}H_{21}NO_2$) C, H, N.

**(−)-3-Deoxymorphine (10).**[36] Compound **10** was made from **5** according to a method previously described by Saá et al.[10a] Formic acid (37 $\mu$L, 0.93 mmol) was added to a stirred mixture of **5** (130 mg, 0.311 mmol), 1,3-bis(diphenylphosphino)-propane (dppp) (20 mg, 46 mmol), $(PPh_3)_2PdCl_2$ (13 mg, 19 mmol), and $(C_4H_9)_3N$ (0.31 mL, 1.3 mmol) in DMF (5 mL). The mixture was stirred for 18 h at 80 °C, the volatiles were evaporated, and the residue was chromatographed [$SiO_2$; $CHCl_3$/MeOH/25% aqueous $NH_3$ (89:10:1)/$CHCl_3$ (60:40)]. The resulting amine was recrystallized from $CH_2Cl_2$−ether to give 76 mg (91%) of pure **10**: mp 227−229 °C (lit.[36] mp 227.5−229 °C); $[\alpha]^{21}_D$ −222.0° (*c* 1.0, MeOH) [lit.[36] −218° (*c* 1.00, MeOH)]; IR (KBr) 3540 cm$^{-1}$ ($\nu$ OH) [IR[36] (Nujol) 3555 cm$^{-1}$ ($\nu$ OH)]; $^1$H NMR ($CDCl_3$) $\delta$ 1.86 (1 H, ddd, $J_{15eq,15ax}$ = 12.6 Hz, $J_{15eq,16ax}$ = 3.7 Hz, $J_{15eq,16eq}$ = 1.8 Hz, H-15eq), 2.07 (1 H, ddd, $J_{15ax,16ax}$ = 12.2 Hz, $J_{15ax,16eq}$ = 5.2 Hz, H-15ax), 2.33 (1 H, dd, $J_{10ax,9}$ = 6.2 Hz, $J_{10ax,10eq}$ = 18.9 Hz, H-10ax), 2.40 (1 H, m, H-16ax), 2.44 (3 H, s, N-C$H_3$), 2.60 (1 H, ddd, $J_{16eq,16ax}$ = 12.3 Hz, H-16eq), 2.68 (1 H, m, H-14), 2.83 (1 H, br s, OH), 3.10 (1 H, app d, H-10eq), 3.36 (1 H, dd, $J_{9,14}$ = 3.3 Hz, H-9), 3.89 (1 H, m, H-6), 4.84 (1 H, dd, $J_{5,6}$ = 6.5 Hz, $J_{5,7}$ = 1.3 Hz, H-5), 5.30 (1 H, ddd, $J_{8,6}$ = 3.3 Hz, $J_{8,7}$ = 9.8 Hz, $J_{8,14}$ = 1.9 Hz, H-8), 5.68 (1 H, m, H-7), 6.58 (1 H, app d, $J_{2,3}$ = 7.9 Hz, H-3), 6.62 (1 H, app d, $J_{1,2}$ = 7.7 Hz, H-1), 7.00 (1 H, dd, H-2); $^{13}$C NMR ($CDCl_3$) $\delta$ 21.1 (C-10), 35.8 (C-15), 40.9 (C-14), 42.2 (C-13), 43.1 (N-*C*$H_3$), 46.4 (C-16), 58.8 (C-9), 66.6 (C-6), 90.7 (C-5), 106.2 (C-3), 119.0 (C-1), 128.2 (C-2), 128.4 (C-8), 129.6, 133.3 (C-7), 135.5, 158.9 (C-4).

**(−)-(*R*)-11-Hydroxyaporphine (2).** Dry nitrogen gas was bubbled through a solution of **10** (49 mg, 0.18 mmol) in concentrated $MeSO_3H$ (3 mL). The mixture was stirred for 15 min at 95 °C and then partitioned between $CHCl_3$ and 10% aqueous $NaHCO_3$. The chloroform layer was dried ($Na_2SO_4$), filtered, and concentrated *in vacuo*. The residue was chro-

matographed [$SiO_2$; $CHCl_3$/MeOH (9:1)]. The crude amine was converted into the hydrochloride and recrystallized twice from MeOH–ether affording 35 mg (67%) of pure **2**·HCl: mp 270 °C dec; $[\alpha]^{22}_D$ −71.6° (*c* 1.0, MeOH); IR (KBr) 3400 (*ν* OH), 2600 $cm^{-1}$ (*ν* $R_3NH^+$); $^1H$ NMR ($CD_3OD$) *δ* 2.88 (1 H, app t, $J_{7\alpha,6a\beta} = J_{7\alpha,7\beta}$ = 14 Hz, H-7α), 3.08–3.18 (1 H, m, H-4), 3.16 (3 H, s, N-C$H_3$), 3.30–3.58 (3 H, m, H-4, H-5, H-7*β*), 3.76–3.82 (1 H, m, H-5), 4.35 (1 H, dd, $J_{6a\beta,7\beta}$ = 3.2 Hz, H-6a*β*), 6.86 (1 H, app d, $J_{10,9}$ = 7.6 Hz, H-10), 6.87 (1 H, app d, $J_{8,9}$ = 7.9 Hz, H-8), 7.11 (1 H, dd, H-9), 7.17 (1 H, app d, $J_{2,3}$ = 7.6 Hz, H-3), 7.35 (1 H, dd, $J_{2,1}$ = 7.9 Hz, H-2), 8.40 (1 H, app d, H-1); $^{13}C$ NMR ($CD_3OD$) *δ* 26.8 (C-4), 33.1 (C-7), 41.9 (N-*C*$H_3$), 53.5 (C-5), 63.6 (C-6), 117.3 (C-10), 120.8 (C-8), 121.2, 127.7, 128.3, 128.9, 129.2, 130.0, 130.3, 133.8, 135.4, 156.2 (C-11). Anal. ($C_{17}H_{18}ClNO$) C, H, N.

Compound **2**·HCl was also synthesized from **8**·HCl by demethylation in 48% aqueous HBr in 74% yield.[7] This method has been used by several other groups for the synthesis of **2** as the hydrobromide salt[3,6] or the free base.[5]

**(−)-(*R*)-11-Hydroxy-10-methylaporphine (3).[5] Method A.** A solution of **7**·HCl (429 mg, 1.36 mmol) in freshly distilled 48% aqueous HBr (30 mL) was stirred for 3.5 h at 120 °C under nitrogen. The volatiles were evaporated, and the residue was partitioned between ether and 10% aqueous $NaHCO_3$. The ether layer was dried ($Na_2SO_4$), filtered, and concentrated *in vacuo*. The resulting oil was chromatographed [$SiO_2$; $CHCl_3$/MeOH (9:1)]. The amine was converted into the hydrochloride and recrystallized from MeOH–ether to give 352 mg (86%) of pure **3**·HCl: mp 271–273 °C dec (lit.[5] mp 270–272 °C dec); $[\alpha]^{21}_D$ −103.4° (*c* 1.0, MeOH); IR (KBr) 3360 (*ν* OH), 2450 $cm^{-1}$ (*ν* $R_3NH^+$); $^1H$ NMR ($CD_3OD$) *δ* 2.27 (3 H, s, Ar-C$H_3$), 2.82 (1 H, app t, $J_{7\alpha,6a\beta} = J_{7\alpha,7\beta}$ = 14 Hz, H-7α), 3.08 (1 H, m, H-4), 3.15 (3 H, s, N-C$H_3$), 3.15–3.45 (3 H, m, H-4, H-5, H-7*β*), 3.74 (1 H, m, H-5), 4.25 (1 H, dd, $J_{6a\beta,7\beta}$ = 2.8 Hz, H-6a*β*), 6.81 (1 H, app d, $J_{8,9}$ = 7.6 Hz, H-8), 7.02 (1 H, d, H-9), 7.16 (1 H, app d, $J_{2,3}$ = 7.6 Hz, H-3), 7.36 (1 H, dd, $J_{1,2}$ = 7.9 Hz, H-2), 8.35 (1 H, app d, H-1); $^{13}C$ NMR ($CD_3OD$) *δ* 17.0 (Ar-*C*$H_3$), 26.7 (C-4), 33.0 (C-7), 41.3 (N-*C*$H_3$), 53.3 (C-5), 63.5 (C-6a), 121.0 (C-8), 122.1, 126.7, 128.2, 128.8, 129.1, 129.3, 130.4, 131.5, 132.9, 134.0, 153.6 (C-11).

**Method B.** A solution of **9** (54 mg, 0.19 mmol) in concentrated $MeSO_3H$ (1 mL) was kept at 95 °C under nitrogen for 1 h. The reaction mixture was partitioned between ether and 10% aqueous $NaHCO_3$. The ether layer was dried ($Na_2SO_4$), filtered, and concentrated *in vacuo*. The oily residue was purified by preparative TLC [$Al_2O_3$; ether/hexane (3:2)]. The amine was converted into the hydrochloride salt, which was recrystallized from MeOH–ether providing 47 mg (82%) of pure **3**·HCl.

**X-ray Analysis of 3·HCl.** Crystals of **3**·HCl were obtained from an ethanol–ether solution, and a crystal with the dimensions 0.50 × 0.10 × 0.02 mm was used for data collection with an Enraf-Nonius CAD4F-11 diffractometer. The angular settings of 25 reflections ($23° < \theta < 47°$) were measured to calculate the lattice parameters, cf Table 1 for crystal data. Intensity data for one unique set of reflections with $\theta < 60°$ ($0 \le h \le 9$, $0 \le k \le 22$, $0 \le l \le 23$) were collected by the $\omega/2\theta$ scan method using monochromatized Cu Kα radiation. Three intensity control reflections, which were measured every 2 h, indicated no significant decay. A total of 2589 reflections were recorded, and of these, 1544 reflections with $I > 2.5\sigma(I)$ were considered observed. All intensities were corrected for Lorentz and polarization effects but not for absorption or extinction.

The structure was solved by direct methods with MITHRIL[37] which provided the non-hydrogen atom positions of the two independent molecules A and B. The positions of hydrogen atoms connected to methyl carbon, nitrogen, or oxygen atoms were determined from $\Delta\rho$ maps. Remaining hydrogen atoms were included at calculated positions. Refinement was carried out by the full-matrix least-squares method using anisotropic temperature factors for the non-hydrogen atoms. The hydrogen atoms were assigned a temperature factor equal to the $U_{eq}$ value of the parent atom. The hydrogen atom parameters were not refined. After refinement the residuals were $R$ = 0.059 and $R_w$ = 0.065 (weights from counting statistics, $S$ = 0.805, $\Delta/\sigma < 0.001$, $-0.27 < \Delta\rho < 0.26$ eÅ$^{-3}$). All calculations have been performed using mainly the program NRCVAX.[38] The molecular conformation and the atom-labeling scheme are shown in Figure 1.

**Computational Methods.** Conformational energies and energy-minimized geometries of the unprotonated amines were obtained on a Macintosh IIfx or Macintosh Centris 650 workstation using the molecular mechanics program MM2(87)[39] or MM2(91)[40] developed by Allinger and co-workers. Conformational energy curves were calculated by using the driver option implemented in MM2(87) with an angle increment of 10° and with full energy minimization except for the dihedral angle(s) used as driving angle(s). The structural modeling was performed by use of the interactive computer graphics program MacMimic, version 2.1, InStar Software, IDEON Research Park, S-233 70 Lund, Sweden.

Semiempirical AM1 calculations were performed using the MOPAC package implemented in Sybyl 6.0.3 (Tripos Associates Inc., 1699 S. Hanley Rd., Suite 303, St Louis, MO). The atomic coordinate files of selected MM2(91)-calculated low-energy conformations of **1**–**3** were imported into Sybyl, converted into the protonated form, and then used as starting points for AM1 calculations. The AM1 calculations were performed with a net charge of 1, full geometrical optimization, and precise ×100 convergence criteria.

All calculations of electrostatic potentials were performed in SPARTAN 3.1.[41] Geometry optimization of selected conformations of **2** and **3** and calculation of electrostatic interactions between the ligands and Gly163 of the 5-$HT_{1A}$ receptor were performed in SPARTAN 3.1 at the RHF/3-21G level with a net charge of 1. A derivative of Gly163 with the C-terminal as an *N*-methyl amide and the N-terminal as an acetamide was used in the calculations.

**Receptor Modeling.** Receptor models were constructed using Sybyl 6.0.3 (Tripos Associates Inc., 1699 S. Hanley Rd., Suite 303, St Louis, MO). The construction of the receptor model for the human 5-$HT_{1A}$ receptor was done by using a strategy which was recently described for the muscarinic m1[18] and dopamine $D_{2A}$ and $D_3$[19] receptors. The 3D-structure of bR[42] was used as template, and the amino acid sequence for the human 5-$HT_{1A}$ receptor was obtained from the published sequence.[20] Energy minimizations were made using Sybyl 6.0.3 and the following parameters: a distance-dependent dielectric constant of 4, a nonbonded cutoff of 9.0, AMBER (kollman all atom or united atom), and conjugated gradient minimization until the rms energy gradient was less than 0.1 kcal/mol Å. Low-energy conformations of **2** and **3** generated by AM1 were used in the binding site modeling.

**Pharmacology. Serotonin 5-$HT_{1A}$ Receptor Binding Assay.** Male Sprague–Dawley rats (weighing about 200 g) were decapitated, and cortex and hippocampus were dissected out. The tissues from each rat were immediately homogenized in 15 mL of ice-cold 50 mM Tris-HCl buffer containing 4.0 mM $CaCl_2$ and 5.7 mM ascorbic acid, pH 7.5, with an UltraTurrax homogenizer for 10 s. After centrifugation for 12.5 min at 17000 rpm (39800*g*), the pellets were resuspended in the same buffer and homogenization and centrifugation repeated. The tissue homogenate was diluted to 8 mg/mL with the buffer, incubated for 10 min at 37 °C, and supplied with 10 *μ*M pargyline followed by reincubation for 10 min.

Incubation mixtures (2 mL) contained various concentrations of test compound (diluted in 50 mM Tris–HCl buffer containing 5.7 mM ascorbic acid, pH 7.5), 2 nM [$^3H$]-8-OH-DPAT·HBr (New England Nuclear, Dreieich, Germany, and Research Biochemicals, Wayland, MA), and 5 mg/mL tissue homogenate in 50 mM Tris-HCl buffer containing 4.0 mM $CaCl_2$ and 5.7 mM ascorbic acid, pH 7.5. Nonspecific binding was measured by the addition of 10 *μ*M 5-HT·HCl to the reaction mixture. Binding experiments were started by the addition of tissue homogenate and followed by incubation at 37 °C for 10 min. The incubations were terminated by rapid filtration through Whatman GF/B glass fiber filters using a Brandel cell harvester. The filters were washed with ice-cold buffer (50 mM Tris-HCl, pH 7.5), and the radioactivity was determined in a Packard 2200CA liquid scintillation analyzer. The binding data were analyzed by nonlinear regression using the LIGAND program.[43]

**Dopamine $D_{2A}$ Receptor Binding Assay.** The dopamine $D_{2A}$ receptor binding assay was performed essentially as described by Malmberg et al.[44] Mouse fibroblast ($Ltk^-$) cells expressing human $D_{2A}$ receptors were obtained from Dr. O. Civelli (Vollum Institute, Portland). The membranes were prepared as described previously,[44] resuspended in binding buffer (in mM: 50 Tris-HCl; 120 NaCl; 1.5 $CaCl_2$; 4 $MgCl_2$; 5 KCl; 1 EDTA; pH 7.4), and stored in aliquots at −70 °C.

The frozen cell membranes were thawed, homogenized with a Branson 450 sonifier, and suspended in binding buffer. The binding assays were performed in a total volume of 0.5 mL with a receptor concentration of about 100 pM. 1 nM [$^3$H]-raclopride (41.5 mCi/mL) was incubated with nonlabeled ligand for 60 min at 22 ± 1 °C. Binding in the presence of (+)-butaclamol (1 μM) was defined as nonspecific. The incubations were terminated, and the radioactivity was determined as described for the 5-$HT_{1A}$ receptor binding assay. The binding curves were analyzed individually by nonlinear regression using the LIGAND program.[43] One- and two-site curve fittings were tested in all experiments, and the two-site model was accepted when it significantly improved the curve fit ($p < 0.05$; $F$-test) and when each site accounted for more than 20% of the receptors.

**Dopamine $D_1$ Receptor Binding Assay.** Membranes were prepared from striatal tissue from male Sprague−Dawley rats as described by Hall et al.[45] The tissue was homogenized and finally resuspended in binding buffer (in mM: 50 Tris-HCl; 120 NaCl; 5 KCl; 2 $CaCl_2$; 1 $MgCl_2$; 5.7 ascorbic acid; 10 μM pargyline; pH 7.6).

The membranes were preincubated in the presence of 40 nM ketanserin for 10 min at 37 °C and suspended in binding buffer to a final concentration of 2.5 mg of original wet weight (about 125 pM receptors)/2 mL. The binding assays were performed with 0.25 nM [$^3$H]SCH23390 (72.8 Ci/mmol) and nonlabeled ligand in a total volume of 2 mL for 60 min at 22 ± 1 °C. Binding in the presence of flupenthixol (1 μM) was defined as nonspecific. The incubations were terminated, and the radioactivity was determined as described for the 5-$HT_{1A}$ receptor binding assay and analyzed as described for the $D_{2A}$ receptor binding assay.

**Forskolin-Stimulated Adenylyl Cyclase Assay. Tissue Preparation.** The conditions used for the tissue preparation were adapted from DeVivo and Maayani.[28] The rats were decapitated, and the brains were removed and chilled in saline (0.9%). The hippocampi were then dissected out rapidly and homogenized in buffer (1:9, original wet wt/vol) containing 300 mM sucrose, 1 mM EGTA, 5 mM EDTA, 20 mM Tris-HCl (pH 7.4), and 5 mM dithiothreitol, using a glass/Teflon homogenizer (20 strokes by hand). The tissue suspension was diluted further 8-fold and centrifuged at 500$g$ for 5 min at 4 °C. The resulting supernatant was centrifuged at 39000$g$ for 10 min. The pellet was stored on ice for no more than 1 h before resuspension in buffer for use in the forskolin-stimulated cyclase assay.

**Assay Conditions.** The 5-HT-sensitive forskolin-stimulated cyclase assay was adapted from DeVivo and Maayani,[29] and the conversion of [α-$^{32}$P]ATP to [α-$^{32}$P]cAMP was quantitated by the method of Salomon.[46] The final composition of the assay medium was 100 mM NaCl, 2 mM $Mg(OAc)_2$, 10 μM forskolin, 80 mM Tris-HCl (pH 7.4), 0.2 mM ATP, 1 mM cAMP, 10 μM GTP, 60 mM sucrose, 4 mM theophylline, 0.2 mM EGTA, 1 mM EDTA, 1 mM dithiothreitol, 0.1 mg/mL creatinine phosphokinase, 5 mM creatinine phosphate, and 1−2 μCi of [α-$^{32}$P]ATP (specific activity, 20−40 Ci/mmol) per sample. Each drug concentration was tested in triplicate. Tubes containing 150 μL of the cyclase assay medium and 50 μL of drug dilution (or water) were preincubated for 5 min at 30 °C, and then the assay was started by the addition of 50 μL of the tissue suspension (100−125 μg of protein per tube). After a 5.25 min incubation at 30 °C, the reaction was terminated by the addition of 100 μL of a solution containing 2% sodium lauryl sulfate, 45 mM ATP, and 1.3 mM cAMP; an internal standard of [$^3$H]cAMP (diluted in water to give approximately 30 000 dpm/50 μL) was added to the samples, and the tubes were subsequently put in a boiling water bath for 3 min. After the samples had cooled to room temperature, the conversion of [α-$^{32}$P]ATP to [α-$^{32}$P]cAMP was quantitated using sequential chromatography. Samples were loaded onto Dowex columns and then eluted with water onto neutral alumina columns. The final fraction of interest (as determined previously from column elution profiles) was eluted from the alumina columns with 0.1 mM imidazole (pH 7.3) directly into scintillation vials containing 10 mL of scintillation fluid (Safety Solve; RPI Corp., Mount Prospect, IL). These samples were then counted in a Packard scintillation counter (B460C) using a program for $^3$H/$^{32}$P dual labeling.

cAMP production was corrected for relative recovery from the columns and expressed as femtomoles of cAMP per minute per microgram of protein or as a fraction of 5-HT-sensitive adenylyl cyclase, as defined by maximal inhibition of forskolin-stimulated cyclase achieved with 10 μM 5-HT. 5-HT routinely inhibited 25−30% of forskolin-stimulated cyclase activity in the rat hippocampal membrane preparation. Protein concentration was measured by the method of Lowry et al.[47] using bovine serum albumine as the standard.

***In Vivo* Microdialysis.** The *in vivo* microdialysis studies were carried out according to methods previously described.[30a,b] Briefly, chloral hydrate-anesthetized male Sprague−Dawley rats (250−350 g; Laboratorietjänst AB, Sollentuna, Sweden) were stereotaxically implanted with U-shaped microdialysis probes into the ventral hippocampus (A-P −4.8, L +4.6, D-V −8.5, reference points bregma and dura[48]). The probes were perfused with artificial CSF containing the 5-HT reuptake inhibitor citalopram (1 μM) and dialysates collected every 20 min for analysis of 5-HT, 5-HIAA, and DOPAC using HPLC (electrochemical detection) methods.[49] Experiments were not commenced until a stable base-line output of 5-HT was established (less than 10% change between consecutive samples); this occurred typically 2−3 h after the probe had been implanted. Compounds **2** and **3** were dissolved in saline and administered sc in a volume of 1 mL/kg of body weight; (−)-pindolol was dissolved in a minimal quantity of glacial HOAc and diluted to volume with saline. (−)-Pindolol was given 40 min before **3** in the interaction experiments.

The absolute average base-line output levels of 5-HT, 5-HIAA, and DOPAC in the present experiments ranged between 44.8 and 68.1 fmol, 4.687 and 6.596 pmol, and 341.5 and 893.0 fmol per 20 μL of dialysate sample, respectively.

The microdialysate levels of 5-HT, 5-HIAA, and DOPAC were expressed as percentages of the absolute amount of the corresponding species in the dialysate collected immediately prior to drug or vehicle administration (= base line), unless stated otherwise. The areas under the curves (AUC) 0−120 min after injection were calculated and used as overall measures of treatment effects. Statistical comparisons between treatments were made on the AUC values using Kruskal−Wallis' ANOVA followed by Mann−Whitney $U$-test. Probability levels of 5% or less were considered statistically significant.

**Acknowledgment.** Skillfull technical assistance by Jessica Schjött in the *in vivo* microdialysis studies and by Anne-Marie Eriksson and Gun Torell-Svantesson in the binding assays is acknowledged. We thank Åsa Malmberg for stimulating discussions regarding the receptor binding assays. Financial support was obtained from the Swedish National Board for Industrial and Technical Development (NUTEK), Astra Arcus, and the Swedish Medical (No. 7486) and Natural (No. 8546) Science Research Council.

**Supplementary Material Available:** Atomic positional and thermal parameters, bond lengths, and bond angles (6 pages). Ordering information is given on any current masthead page.

## References

(1) Matthiessen, A.; Wright, C. R. A. *Proc. R. Soc. London, Ser. B* **1869**, *17*, 455.

(2) (a) Goldman, M. E.; Kebabian, J. W. Aporphine enantiomers. Interactions with D-1 and D-2 dopamine receptors. *Mol. Pharmacol.* **1984**, *25*, 18–23. (b) Baldessarini, R. J.; Kula, N. S.; Zong, R.; Neumeyer, J. L. Receptor affinities of aporphine enantiomers in rat brain tissue. *Eur. J. Pharmacol.* **1994**, *254*, 199–203.

(3) Schaus, J. M.; Titus, R. D.; Foreman, M. M.; Mason, N. R.; Truex, L. L. Aporphines as antagonists of dopamine receptors. *J. Med. Chem.* **1990**, *33*, 600–607.

(4) Neumeyer, J. L.; Granchelli, F. E.; Fuxe, K.; Ungerstedt, U.; Corrodi, H. Aporphines. 11. Synthesis and dopaminergic activity of monohydroxyaporphines. Total synthesis of (±)-11-hydroxyaporphine, (±)-11-hydroxynoraporphine, and (±)-11-hydroxy-*N*-*n*-propylnoraporphine. *J. Med. Chem.* **1974**, *17*, 1090–1095.

(5) Cannon, J. G.; Mohan, P.; Bojarski, J.; Long, J. P.; Bhatnagar, R. K.; Leonard, P. A.; Flynn, J. R.; Chatterjee, T. K. (*R*)-10-Methyl-11-hydroxyaporphine: A highly selective serotonergic agonist. *J. Med. Chem.* **1988**, *31*, 313–318.

(6) Ram, V. J.; Neumeyer, J. L. Aporphines. 42. Synthesis of (*R*)-(−)-11-hydroxyaporphines from morphine. *J. Org. Chem.* **1982**, *47*, 4372–4374.

(7) Hedberg, M. H.; Johansson, A. M.; Hacksell, U. Facile syntheses of aporphine derivatives. *J. Chem. Soc., Chem. Commun.* **1992**, 845–846.

(8) Echavarren, A. M.; Stille, J. K. Palladium-catalyzed coupling of aryl triflates with organostannanes. *J. Am. Chem. Soc.* **1987**, *109*, 5478–5486.

(9) (a) Murahashi, S.-I.; Hirano, T.; Yano, T. Palladium catalyzed amine exchange reaction of tertiary amines. Insertion of palladium(0) into carbon-hydrogen bonds. *J. Am. Chem. Soc.* **1978**, *100*, 348–350. (b) Murahashi, S.-I.; Watanabe, T. Palladium catalyzed hydrolysis of tertiary amines with water. *J. Am. Chem. Soc.* **1979**, *101*, 7429–7430. (c) McCrindle, R.; Ferguson, G.; Arsenault, G. J.; McAlees, A. J.; Stephenson, D. K. Formation and characterisation of enamine complexes of palladium(II) chloride. crystal structure analysis of di-$\mu$-chlorobis[2-(*NN*-diisopropylimino)ethyl-*C*]-dipalladium(II). *J. Chem. Res., Symp.* **1984**, 360–361. (d) Cabri, W.; Candiani, I.; DeBernardinis, S.; Francalanci, F.; Penco, S. Heck reaction on anthraquinone derivatives: ligand, solvent, and salt effects. *J. Org. Chem.* **1991**, *56*, 5796–5800.

(10) For examples of palladium-catalyzed reductions using a trialkylamine as hydride source, see: (a) Saá, J. M.; Dopico, M.; Martorell, G.; García-Raso, A. Deoxygenation of highly hindered phenols. *J. Org. Chem.* **1990**, *55*, 991–995. (b) Stokker, G. E. Palladium catalyzed stereospecific Michael arylation of 6-alkyl-5,6-dihydro-2*H*-pyran-2-ones. *Tetrahedron Lett.* **1987**, *28*, 3179–3182.

(11) (a) Martorell, G.; García-Raso, A.; Saá, J. M. Palladium catalyzed cross-coupling of phenol triflates with organostannanes. A versatile approach for the synthesis of substituted resorcinol dimethyl ethers. *Tetrahedron Lett.* **1990**, *31*, 2357–2360. (b) Saá, J. M.; Martorell, G.; García-Raso, A. Palladium-catalyzed cross-coupling reactions of highly hindered, electron-rich phenol triflates and organostannanes. *J. Org. Chem.* **1992**, *57*, 678–685.

(12) Giesecke, J. The crystal and molecular structure of apomorphine hydrochloride hydrate. *Acta Crystallogr.* **1973**, *29*, 1785–1791.

(13) (a) Johansson, A. M.; Karlén, A.; Grol, C. J.; Sundell, S.; Kenne, L.; Hacksell, U. Dopaminergic 2-aminotetralins: affinities for dopamine $D_2$-receptors, molecular structures, and conformational preferences. *Mol. Pharmacol.* **1986**, *30*, 258–269. (b) Liljefors, T.; Wikström, H. A. molecular mechanics approach to the understanding of presynaptic selectivity for centrally acting dopamine receptor agonists of the phenylpiperidine series. *J. Med. Chem.* **1986**, *29*, 1896–1904. (c) Froimowitz, M.; Neumeyer, J. L.; Baldessarini, R. J. A stereochemical explanation of the dopamine agonist and antagonist activity of stereoisomeric pairs. *J. Med. Chem.* **1986**, *29*, 1570–1573.

(14) Cahn, R. S.; Ingold, C.; Prelog, V. Spezifikation der molekularen chiralität. (Specification of molecular chirality). *Angew. Chem.* **1966**, *78*, 413–447.

(15) Jansen, J. M.; Karlén, A.; Grol, C. J.; Hacksell, U. Conformational properties of melatonin and two conformationally restricted agonists: A molecular mechanics and NMR spectroscopic study. *Drug Des. Discovery* **1993**, *10*, 115–133.

(16) Wikström, H.; Lii, J.-H.; Allinger, N. The dopaminergic moiety of the ergots: A controversial topic studied with molecular mechanics. *J. Med. Chem.* **1987**, *30*, 1928–1934.

(17) The difference in amino acid composition of the transmembrane regions between the human and rat 5-$HT_{1A}$ receptor is only one amino acid residue.

(18) Nordvall, G.; Hacksell, U. Binding-site modeling of the muscarinic m1 receptor: A combination of homology-based and indirect approaches. *J. Med. Chem.* **1993**, *36*, 967–976.

(19) Malmberg, Å.; Nordvall, G.; Johansson, A. M.; Mohell, N.; Hacksell, U. Molecular basis for the binding of 2-aminotetralins to human dopamine $D_{2A}$ and $D_3$ receptors. *Mol. Pharmacol.* **1994**, *46*, 299–312.

(20) (a) Kobilka, B. K.; Frielle, T.; Collins, S.; Yang-Feng, T.; Kobilka, T. S.; Francke, U.; Lefkowitz, R. J.; Caron, M. G. An intronless gene encoding a potential member of the family of receptors coupled to guanine nucleotide regulatory proteins. *Nature* **1987**, *329*, 75–79. (b) Fargin, A.; Raymond, J. R.; Lohse, M. J.; Kobilka, B. K.; Caron, M. G.; Lefkowitz, R. J. The genomic clone G-21 which resembles a $\beta$-adrenergic receptor sequence encodes the 5-$HT_{1A}$ receptor. *Nature* **1988**, *335*, 358–360.

(21) (a) Trumpp-Kallmeyer, S.; Hoflack, J.; Bruinvels, A.; Hibert, M. Modeling of G-protein-coupled receptors: Application to dopamine, adrenaline, serotonin, acetylcholine, and mammalian opsin receptors. *J. Med. Chem.* **1992**, *35*, 3448–3462. (b) Sylte, I.; Edvardsen, O.; Dahl, S. G. Molecular dynamics of the 5-HT(1a) receptor and ligands. *Protein Eng.* **1993**, *6*, 691–700. (c) Kuipers, W.; Van Wijngaarden, I.; IJzerman, A. P. A model of the serotonin 5-$HT_{1A}$ receptor: Agonist and antagonist binding sites. *Drug Des. Discovery* **1994**, *11*, 231–249. (d) Dijkstra, G. D. H.; Tulp, M. Th. M.; Hermkens, P. H. H.; van Maarseveen, J. H.; Scheeren, H. W.; Kruse, C. G. Synthesis and receptor-affinity profile of *N*-hydroxytryptamine derivatives for serotonin and tryptamine receptors. A molecular-modelling study. *Recl. Trav. Chim. Pays-Bas* **1993**, *112*, 131–136.

(22) Mellin, C.; Vallgårda, J.; Nelson, D. L.; Björk, L.; Yu, H.; Andén, N.-E.; Csöregh, I.; Arvidsson, L.-E.; Hacksell, U. A 3-D model for 5-$HT_{1A}$-receptor agonists based on stereoselective methyl-substituted and conformationally restricted analogues of 8-hydroxy-2-(dipropylamino)tetralin. *J. Med. Chem.* **1991**, *34*, 497–510.

(23) Nordvall, G. Unpublished results.

(24) (a) Chanda, P. K.; Minchin, M. C. W.; Davis, A. R.; Greenberg, L.; Reilly, Y.; McGregor, W. H.; Bhat, R.; Lubeck, M. D.; Mizutani, S.; Hung, P. P. Identification of residues important for ligand binding to the human 5-hydroxytryptamine$_{1A}$ serotonin receptor. *Mol. Pharmacol.* **1993**, *43*, 516–520. (b) Ho, B. Y.; Karschin, A.; Branchek, T.; Davidson, N.; Lester, H. A. The role of conserved aspartate and serine residues in ligand binding and in function of the 5-$HT_{1A}$ receptor - A site-directed mutation study. *FEBS Lett.* **1992**, *312*, 259–262.

(25) (a) Strader, C. D.; Sigal, I. S.; Register, R. B.; Candelore, M. R.; Rands, E.; Dixon, R. A. F. Identification of residues required for ligand binding to the beta-adrenergic receptor. *Proc. Natl. Acad. Sci. U.S.A.* **1987**, *84*, 4384–4388. (b) Wang, C. D.; Buck, M. A.; Fraser, C. M. Site-directed mutagenesis of $\alpha_{2A}$-adrenergic receptors-identification of amino acids involved in ligand binding and receptor activation by agonists. *Mol. Pharmacol.* **1991**, *40*, 168–179.

(26) (a) Neve, K. A.; Cox, B. A.; Henningsen, R. A.; Spanoyannis, A.; Neve, R. L. Pivotal role for aspartate-80 in the regulation of dopamine D2 receptor affinity for drugs and inhibition of adenylyl cyclase. *Mol. Pharmacol.* **1991**, *39*, 733–739. (b) Horstman, D. A.; Brandon, S.; Wilson, A. L.; Guyer, C. A.; Cragoe, E. J., Jr.; Limbird, L. E. An aspartate conserved among G-protein receptors confers allosteric regulation of $\alpha$2-adrenergic receptors by sodium. *J. Biol. Chem.* **1990**, *265*, 21590–21595.

(27) Cox, B. A.; Henningsen, R. A.; Spanoyannis, A.; Neve, R. L.; Neve, K. A. Contributions of conserved serine residues in the interactions of ligands with dopamine $D_2$ receptors. *J. Neurochem.* **1992**, *59*, 627–635.

(28) (a) Seeman, P.; Ulpian, C.; Grigoriadis, D.; Pri-Bar, I.; Buchman, O. Conversion of dopamine $D_1$ receptors from high to low affinity for dopamine. *Biochem. Pharmacol.* **1985**, *34*, 151–154. (b) Grigoriadis, D.; Seeman, P. Complete conversion of brain $D_2$ dopamine receptors from the high- to the low-affinity state for dopamine agonists, using sodium ions and guanine nucleotide. *J. Neurochem.* **1985**, *44*, 1925–1935.

(29) DeVivo, M.; Maayani, S. Characterization of the 5-hydroxytryptamine$_{1A}$ receptor-mediated inhibition of forskolin-stimulated adenylyl cyclase activity in guinea pig and rat hippocampal membranes. *J. Pharmacol. Exp. Ther.* **1986**, *238*, 248–253.

(30) (a) Sharp, T.; Bramwell, S. R.; Clark, D.; Grahame-Smith, D. G. In vivo measurement of extracellular 5-hydroxytryptamine in hippocampus of the anesthetized rat using microdialysis: Changes in relation to 5-hydroxytryptaminergic neuronal activity. *J. Neurochem.* **1989**, *53*, 234–240. (b) Hjorth, S.; Sharp, T.; Liu, Y. *Cis*-(+)-8-OH-1-$CH_3$-DPAT, (+)-ALK-3, a novel stereoselective pharmacological probe for characterizing 5-HT release-controlling 5-$HT_{1A}$ autoreceptors. An *in vivo* brain microdialysis study. *Naunyn-Schmiedeberg's Arch. Pharmacol.* **1990**, *341*, 149–157. (c) Vahabzadeh, A.; Fillenz, M. Studies on the origin of rat hippocampal dihydroxyphenylacetic acid using microdialysis. *Neurosci. Lett.* **1992**, *136*, 51–55.

(31) Björk, L.; Cornfield, L. J.; Nelson, D. L.; Hillver, S.-E.; Andén, N.-E.; Lewander, T.; Hacksell, U. Pharmacology of the novel 5-hydroxytryptamine$_{1A}$ receptor antagonist (*S*)-5-fluoro-8-hydroxy-2-(dipropylamino)tetralin: Inhibition of (*R*)-8-hydroxy-2-(dipropylamino)tetralin-induced effects. *J. Pharmacol. Exp. Ther.* **1991**, *258*, 58–65.

(32) Assignments of signals in $^1$H-NMR spectra of the novel morphine analogues were compared with data published for 3-*O*-acetylmorphine in $CDCl_3$: Neville, G. A.; Ekiel, I. and Smith, I. C. P. High-resolution proton magnetic resonance spectra of morphine and its three *O*-acetyl derivatives. *Magn. Reson. Chem.* **1987**, *25*, 31–35.
(33) Assignments of signals in $^{13}$C NMR-spectra of the novel morphine derivatives were compared to data published for codeine and 3-*O*-acetylmorphine in $CDCl_3$; see: Carroll, F. I.; Moreland, C. G.; Brine, G. A.; Kepler, J. A. Carbon-13 nuclear magnetic resonance spectra of morphine alkaloids. *J. Org. Chem.* **1976**, *41*, 996–1001.
(34) Cannon, J. G.; Moe, S. T.; Long, J. P. Enantiomers of 11-hydroxy-10-methylaporphine having opposing pharmacological effects at 5-$HT_{1A}$ receptors. *Chirality* **1991**, *3*, 19–23.
(35) Cacchi, S.; Ciattini, P. G.; Morera, E.; Ortar, G. Palladium-catalyzed triethylammonium formate reduction of aryl triflates. A selective method for the deoxygenation of phenols. *Tetrahedron Lett.* **1986**, *27*, 5541–5144.
(36) Reden, J.; Reich, M. F.; Rice, K. C.; Jacobson, A. E.; Brossi, A. Deoxymorphines: Role of the phenolic hydroxyl in antinociception and opiate receptor interactions. *J. Med. Chem.* **1979**, *22*, 256–259.
(37) Gilmore, C. J. MITHRIL-an integrated direct-methods computer program. *J. Appl. Crystallogr.* **1984**, *17*, 42–46.
(38) Gabe, E. J.; LePage, Y.; Charland, J.-P.; Lee, F. L.; White, P. S. NRCVAX-an interactive program system for structure analysis. *J. Appl. Crystallogr.* **1989**, *22*, 384–387.
(39) Sprague, J. T.; Tai, J. C.; Yuh, Y.; Allinger, N. L. The MMP2 calculational method. *J. Comput. Chem.* **1987**, *8*, 581–603.
(40) (a) Allinger, N. L.; Yuh, Y. *Quantum Chemistry Program Exchange* **1980**, *12*, 395. (b) Burkert, U.; Allinger, N. L. *Molecular Mechanics*; American Chemical Society: Washington, DC, 1982.
(41) Wavefunction Inc., 18401 Von Karman Ave., Suite 370, Irvine, CA 92715.
(42) Henderson, R.; Baldwin, J. M.; Ceska, T. A.; Zemlin, F.; Beckmann, E.; Downing, K. H. Model for the structure of bacteriorhodopsin based on high-resolution electron cryomicroscopy. *J. Mol. Biol.* **1990**, *213*, 899–929.
(43) Munson, P. J.; Rodbard, D. LIGAND: A versatile computerized approach for characterization of ligand-binding systems. *Anal. Biochem.* **1980**, *107*, 220–239.
(44) Malmberg, Å.; Jackson, D. M.; Eriksson, A.; Mohell, N. Unique binding characteristics of antipsychotic agents interacting with human dopamine $D_{2A}$, $D_{2B}$, and $D_3$ receptors. *Mol. Pharmacol.* **1993**, *43*, 749–754.
(45) Hall, H.; Sällemark, M.; Jerning, E. Effects of remoxipride and some related new substituted salicylamides on rat brain receptors. *Acta Pharmacol. Toxicol.* **1986**, *58*, 61–70.
(46) Salomon, Y. Adenylyl cyclase assay. *Adv. Cyclic Nucleotide Res.* **1979**, *10*, 35–55.
(47) Lowry, O. H.; Rosebrough, N. J.; Farr, A. L.; Randall, R. J. Protein measurement with the folin phenol reagent. *J. Biol. Chem.* **1951**, *193*, 265–275.
(48) Paxinos, S.; Watson, C. *The rat brain in stereotaxic coordinates*; Academic Press: Sydney, 1982.
(49) Tao, R.; Hjorth, S. α2-Adrenoceptor modulation of 5-hydroxytryptamine release in rat ventral hippocampus in vivo. *Naunyn-Schmiedeberg's Arch. Pharmacol.* **1992**, *345*, 137–143.

JM9406357